PNNL-15103

Pacific Northwest
National Laboratory
Operated by Battelle for the
U.S. Department of Energy

Long Wave Infrared Cavity Enhanced Sensors

M. S. Taubman
D. C. Scott
B. D. Cannon
T. L. Myers
C. A. Bonebrake
P. M. Aker
M. D. Wojcik
J. T. Munley
V. T. Nguyen
J. F. Schultz

October 2004

Prepared for the U.S. Department of Energy
under Contract DE-AC05-76RL01830

DISCLAIMER

PACIFIC NORTHWEST NATIONAL LABORATORY
operated by
BATTELLE
for the
UNITED STATES DEPARTMENT OF ENERGY
under Contract DE-AC05-76RL01830

Printed in the United States of America

Available to DOE and DOE contractors from the
Office of Scientific and Technical Information,
P.O. Box 62, Oak Ridge, TN 37831-0062;
ph: (865) 576-8401
fax: (865) 576-5728
email: reports@adonis.osti.gov

Available to the public from the National Technical Information Service,
U.S. Department of Commerce, 5285 Port Royal Rd., Springfield, VA 22161
ph: (800) 553-6847
fax: (703) 605-6900
email: orders@ntis.fedworld.gov
online ordering: http://www.ntis.gov/ordering.htm

This document was printed on recycled paper.
(9/2003)

PNNL-15103

Long Wave Infrared Cavity Enhanced Sensors

M. S. Taubman
D. C. Scott
B. D. Cannon
T. L. Myers
C. A. Bonebrake
P. M. Aker
M. D. Wojcik
J. T. Munley
V. T. Nguyen
J. F. Schultz

October 2004

Prepared for
the U.S. Department of Energy
under Contract DE-AC05-76RLO1830

Pacific Northwest National Laboratory
Richland, Washington 99352

Summary

The principal goal of Pacific Northwest National Laboratory's (PNNL's) long wave infrared (LWIR) cavity enhanced sensor (CES) project is to explore ultra-sensitive spectroscopic techniques and apply them to the development of LWIR chemical sensors needed for detecting weapons proliferation. This includes detecting not only the weapons of mass destruction (WMDs) themselves, but also signatures of their production and/or detonation. The LWIR CES project is concerned exclusively with developing point sensors; other portions of PNNL's IR Sensors program address stand off detection. PNNL's LWIR CES research is distinguished from that done by others by the use quantum cascade lasers (QCLs) as the light source. QCLs are novel devices, and a significant fraction of our research has been devoted to developing the procedures and hardware required to implement them most effectively for chemical sensing. This report details the progress we have made on our LWIR CES sensor development.

During FY02, PNNL investigated three LWIR CES implementations beginning with the easiest to implement, direct cavity-enhanced detection (simple CES), including a technique of intermediate difficulty, cavity-dithered phase-sensitive detection (FM recovery CES) through to the most complex technique, that of resonant sideband cavity-enhanced detection also known as noise-immune cavity-enhanced optical heterodyne molecular spectroscopy, or NICE-OHMS. This latter technique proved the most sensitive, with confirmed values of 9.7×10^{-11} cm^{-1} $(Hz)^{-1/2}$ being observed, which is within a factor of 20 of the theoretical shot noise limit of 4.9×10^{-12} cm^{-1} $(Hz)^{-1/2}$.

After attempts to improve instrument sensitivity in FY03, the optimum architecture for a fieldable LWIR CES became clear. Problems with reproducibly modulating the QCLs at the high frequencies necessary for NICE-OHMS, and the accompanying reduction in detector sensitivity at these frequencies, indicated that lower frequency operation was desirable. This caused us to choose the intermediate technique of the FM recovery over the resonant sideband technique of NICE-OHMS for the near term. In FY02 and FY03, we also explored the use of the sub-Doppler features known as Lamb dips, in order to increase both sensitivity and selectivity. At the low pressures required for the observation of such features however (10 milliTorr or less), typical LWIR-absorbing analytes saturate heavily even at the moderate operating powers experienced inside the optical cavities employed in the current experiments, resulting in loss of signal and thus sensitivity. Operation at higher pressures (1 to 10 Torr) reduces these saturation effects, by redistributing the upper and lower populations via collisional broadening. However, this also washes out any narrow features such as Lamb dips, indicating that Doppler-limited spectroscopy was the best recourse when operating at these higher pressures. The resulting sensor choice was the intermediate technique of the FM recovery CES, operating in the Doppler-limited regime at moderate pressures of a few Torr or so. This technique offers considerable sensitivity gains over the simple CES, but does not suffer from the complexity and fine tuning requirements of the full NICE-OHMS technique.

FY04 has seen extensive planning and infrastructure development necessary for the experimental work using the FM recovery architecture. For this second phase of LWIR cavity-enhanced experimental work, an entirely separate experiment is being constructed. Considerable effort has been invested in selecting test gases suitable both for laboratory and field experiments. This has involved selection of specific lines, sufficiently free of interference from ubiquitous atmospheric components such as water and

carbon dioxide. As some of these selected gases are hazardous, the laboratory has been modified to ensure no threat is posed to its occupants. Once the molecular transitions were selected, suitable lasers were ordered from our supplier, Maxion technologies. Improvements have also been made to existing components, including laser mounting and related vacuum systems and laser drive electronics.

Contents

Summary iii

1.0 Introduction 1.1

1.1 Summary of Investigated Sensors 1.1
1.2 Discussion of FY03 Conclusions 1.4
1.3 Summary of Progress During FY04 ..... 1.6

2.0 Selection of Test Molecules and Laser Wavelengths 2.1

2.1 Summary of Test Molecules and Laser Wavelengths 2.1
2.1.1 Ammonia (NH_3) 2.1
2.1.2 Nitrous Oxide (N_2O) 2.3
2.1.3 Nitric Oxide (NO) and Nitrogen Dioxide (NO_2) 2.4
2.2 Summary of Selected Laser Lines 2.5

3.0 Modifications to Equipment 3.1

3.1 Laser Dewars 3.1
3.2 Laser Mounts 3.4
3.3 Vacuum Systems, Manifolds, and Purging Requirements 3.6

4.0 Optimization of QCL Current Supply 4.1

4.1 Stability of Main Regulator and Cascode Blocks 4.2
4.2 Noise of Cascode Blocks, a Question of Which Transistor 4.3
4.3 Long-term Stability and Reference Drift 4.5
4.4 Output Filtering, Resulting Resonances 4.5

5.0 Plans for FY05 ..... 5.1

5.1 Optimizing FM Dither Technique 5.2
5.2 The Next Step in Stabilization 5.2
5.3 Reducing the Footprint, and the Option of a Ring Cavity 5.3

6.0 Summary and Outlook 6.1

7.0 References 7.1

Figures

1.1 Cavity-Stabilized QCL Used as a Chemical Sensor 1.2

1.2 FM Recovery Cavity-Enhanced Sensor 1.2

1.3 NICE-OHMS Recovery Sensor 1.3

1.4 Sequence of Intra-Cavity Lamb Dips for Various Saturation Levels 1.5

2.1 Spectrum of Ammonia Comparing SWIR and LWIR Absorption Levels 2.2

2.2a Choice of Specific Ammonia Line by FM Dial Researchers at PNNL. 2.2

2.2b Zoom of the Line in 2.2a. 2.2

2.3a Spectrum of N_2O P-Branch at 1271 cm^{-1}, Showing Water Interference 2.4

2.3b Zoom of a Specific Component of Spectrum Shown in 2.4a, clear of Water Lines. 2.4

2.4a Spectrum of N_2O P-Branch at 1271 cm^{-1}, Showing Lack of Water Interference. 2.4

2.4b Zoom of a Specific Component of Spectrum Shown in 2.6a, Clear of Water Lines. 2.4

3.1a QCL Cryogenic Laser Dewar Made by K-Dell for Laser Components. 3.1

3.1b Cutaway View of Laser Dewar Shown in Figure 3.1a. 3.1

3.2a K-Dell Dewar Modified by PNNL Showing Custom Extended Outer Housing. 3.3

3.2b Cutaway View of the PNNL-Modified K-Dell Dewar. 3.3

3.3 Photograph of the Modified Dewar Components Before Assembly 3.4

3.4 View of K-Dell Dewar with Laser Mounted to Cold Plate 3.5

3.5 New QCL Mount, Allowing Better Access and Thermal Conduction 3.6

3.6 Mixing Manifold Installed on the LeyBold Pumping Station 3.7

4.1 Simplified Schematic of the QCL Current Controller 4.2

4.2a Current Noise Comparison of Transistors 2N3904 and 2N2222A 4.4

4.2b Voltage Noise Comparison of Transistors 2N3904 and 2N2222A 4.4

4.3a Voltage Noise Levels in Cascode Circuit Employing 2N3904 Transistor 4.5

4.3b Voltage Noise Levels in Cascode Circuit Employing 2N2222A Transistor 4.5

4.4 Transfer Function of Fast Input Network 4.6

5.1 FM Recovery Cavity-Enhanced Sensor showing Areas of Focus 5.1

5.2 Cut-away Views of the Original Piezo Mount 5.2

5.3 Cut-away Views of Modified Piezo Mount 5.3

5.4 Ring Cavity Version of the FM Recovery Sensor. 5.4

Table

2.1 Summary of Chosen Laser Frequencies and Wavelengths. 2.5

1.0 Introduction

Various CES architectures were examined during FY02 and FY03. Various operational limitations were discussed in detail in the FY03 report. The brief summary of these architectures given in the FY03 report is reproduced here for the readers' convenience, and then the findings in the FY03 report are summarized.

1.1 Summary of Investigated Sensors

The most basic cavity-enhanced sensor we tested is shown in Figure 1.1. It is referred to as the "Simple Cavity-Enhanced Sensor", since it is based on direct transmission through the optical cavity, without the use of any modulation technique other than that involved in locking the laser to the optical cavity. The optical field from a quantum cascade laser (QCL) is coupled into an optical cavity via an acousto-optic modulator (AOM) and a Faraday isolator in order to minimize the optical feedback into the QCL from back reflections. Reflected and transmitted light from the cavity are observed using detectors D1 and D2 respectively. The QCL is locked to the optical cavity using the Pound-Drever-Hall (PDH) technique, the electronics for this being compressed into one block called "stabilization electronics." The optical cavity also forms a chamber allowing an analyte to be introduced at low pressures. A piezoelectric element in contact with the transmission mirror allows the optical cavity length to be scanned, thus changing the cavity mode frequencies and that of the QCL since it is locked to one of these modes. As the frequency of the sensor is scanned, the signal from detector D2, is filtered at some bandwidth B, measured on an oscilloscope and then recorded.

The advantages of this sensor are that its operation is relatively simple, and it gives a direct result that can exactly be modeled mathematically. Because of this, it is an extremely useful tool for measuring absorption and saturation values of various test analytes. The disadvantages are that the sensitivity is directly limited by the low frequency amplitude noise of the laser and detector, specifically, "1-over-f" or 1/f noise.

The next kind of sensor we use is the "FM Recovery Cavity-Enhanced Sensor", shown in Figure 1.2. Here, a modulation technique is added to reduce the impact of the low frequency noise mentioned above. Again, the QCL is locked to the peak of the cavity mode and the cavity length is scanned or swept to move both mode and laser frequency across molecular absorption features. The difference is that in addition to be being scanned, the cavity length is also rapidly "dithered" using a modulation frequency in the 10s of kHz. This cavity modulation signal (independent of that applied to the laser in order to lock it to the cavity), is applied directly to the piezoelectric element in addition to the signal used to produce the frequency sweep. Since this modulation frequency is well within the bandwidth of the laser-locking loop, the laser frequency follows this cavity dither in the same way as it follows a cavity sweep. The signal from the transmission detector is then demodulated at this dither frequency, after which, it is filtered and recorded on a digital oscilloscope as before.

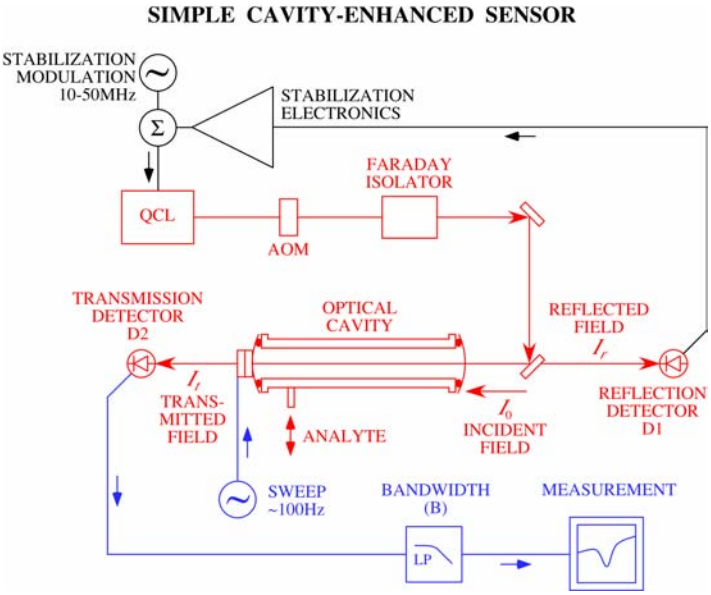

Figure 1.1. Cavity-Stabilized QCL Used as a Chemical Sensor. Absorption due to the intra-cavity analyte causes dramatic changes in the cavity transmission. Optical elements are in red, stabilization in black, measurement electronics in blue. Incident, reflected and transmitted cavity fields of intensities I_0, I_r and I_t are indicated.

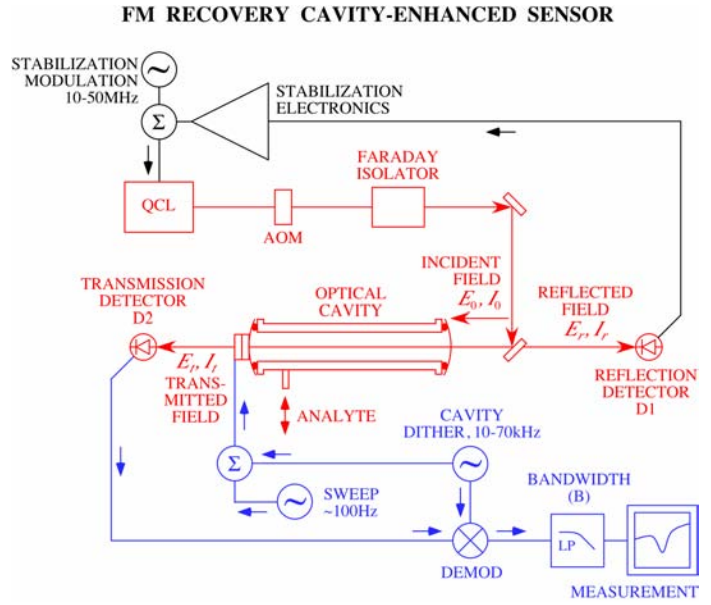

Figure 1.2. FM Recovery Cavity-Enhanced Sensor. The QCL is locked to the cavity as before. However, in addition to the cavity length being scanned, it is also dithered or modulated. The transmission signal from D2 is demodulated accordingly, then filtered and recorded as before. Intensities and electric field amplitudes are indicated for incident, reflected and transmitted fields.

The main advantage of this dithered cavity sensor is that the cavity dither encodes the absorption information onto the light at a frequency above the regions where 1/f noise dominate, thus increasing the resulting signal to noise of the sensor. Demodulation of the signal seen at detector D2 at this cavity modulation frequency then decodes the information, and derivative-like absorption features can be obtained. Another advantage is that this technique is sensitive to spectral features of a specific width, and hence the modulation depth can be adjusted to target certain features.

The disadvantage of this sensor is a slight increase in complexity. The modulation technique requires a source, the piezoelectric behavior needs to be understood, and the sensor needs to be more carefully optimized. However, these disadvantages are relatively minor in comparison to the benefits of this sensor.

The next step in the development of cavity-enhanced sensors was to use the technique of resonant sideband detection, or NICE-OHMS (Ye, Ma, and Hall 1998; Gianfrani, Fox, and Hollberg 1999; Ishibashi and Sasada 1999). Figure 1.3 shows the NICE-OHMS experimental arrangement. In addition to the modulation required for the locking of the QCL to the optical cavity, a modulation is applied at the cavity free spectral range (FSR – the frequency interval between consecutive cavity modes), which was 387.5 MHz for these experiments. The resulting sidebands on the incident field coincide exactly with separate optical cavity modes and thus enter the optical cavity in addition to the carrier. The field transmitted from the cavity is detected and demodulated first at this high frequency, and then at the

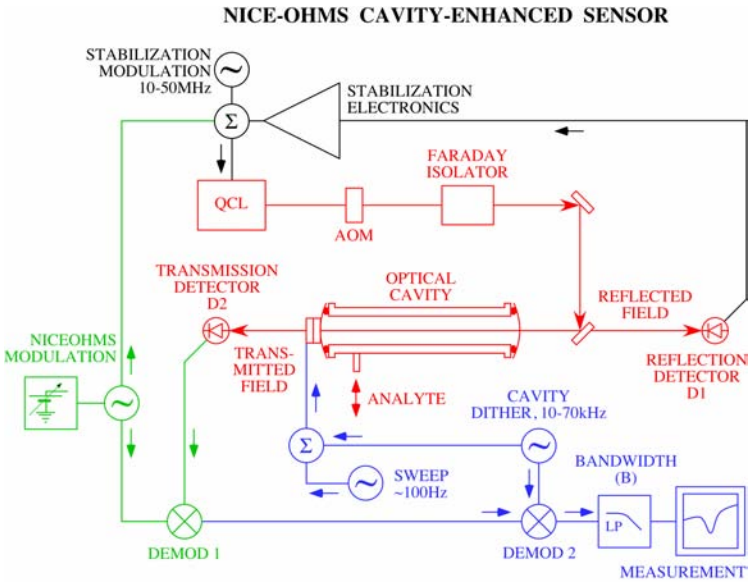

Figure 1.3. NICE-OHMS Recovery Sensor. A high frequency modulation is imposed on the laser in addition to that required for the cavity locking. This high frequency is equal to the spacing between adjacent cavity modes. The resulting transmission signal is first demodulated at this frequency, then secondly at the cavity modulation frequency as explained for the FM recovery cavity-enhanced sensor.

cavity-dither modulation frequency, these processes being represented by DEMOD1 and DEMOD2 respectively. The resulting signal is then filtered at some bandwidth and monitored during cavity scans as before.

The NICE-OHMS sensor configuration shown here potentially has the best performance of all the presented techniques. To begin with, the resonant sideband technique gives immunity to noise in the lock between the QCL and the optical cavity, becoming more important if cavities with very high finesse are used, which are harder to lock a laser to. The high frequency modulation required to achieve NICE-OHMS results in the FM detection occurring at a frequency where the technical noise on the laser is virtually non-existent, giving the best possible immunity to 1/f noise. The cavity-dither technique also employed here allows the selectivity of the instrument to be increased as previously discussed. The result is an instrument with highly optimized sensitivity and selectivity.

While this technique promises a lot, it is considerably more complex. It requires careful matching between cavity length and modulation frequency, which, while not being so extreme as to require an automated system, can be a problem at first (or any subsequent recalibration), because no signal is seen until the matching is reasonably close. Also, the detectors available at these wavelengths do not perform well at high frequencies resulting in considerable loss of signal, and the modulation characteristics of QCLs at these frequencies have not been found to be uniform.

1.2 Discussion of FY03 Conclusions

During FY03, several limitations were discovered pertaining both to the use of high frequency modulation and detection in the LWIR with QCL-based CES, and the use of sub-Doppler spectroscopic techniques in high finesse optical cavities. While not so severe that they justify halting research into these areas, it was clear that they limit the applicability of both the NICE-OHMS technique and the use of sub-Doppler features for the development of fieldable sensors in the LWIR at this time. For this reason the techniques of direct cavity transmission detection and Doppler-limited FM recovery, using Doppler-limited spectroscopy, were chosen as viable fieldable technologies.

The first and most profound limitation was that of saturation when observing the sub-Doppler features known as Lamb dips, as shown in Figure 1.4. When molecular transitions are pumped hard enough so that the excitation rate is faster than the thermalization rates via collisions, spontaneous emission and other processes, the upper levels become significantly populated. This causes stimulated emission to compete with the absorption process, and causes the effective absorption of the medium to decrease. At low levels, this results in the appearance of sub-Doppler features, which in principle offer increased selectivity and sensitivity. At high levels however, the result can be a large reduction in absorption, and thus signal and sensitivity. At an extreme, it can even result in complete transparency of the medium. To understand saturation and sub-Doppler features, we consider the thermal distribution of velocities along the longitudinal axis of the optical cavity. Molecules with different velocities interact with the optical field at different frequencies due to the effect of the Doppler shift. This gives rise to a Gaussian broadening of spectral features, known as the “Doppler profile”. Also, molecules moving with some speed along this axis interact only with the optical field propagating in one direction: the Doppler-shifted frequency of the counter-propagating field is too far detuned. However, molecules with relatively

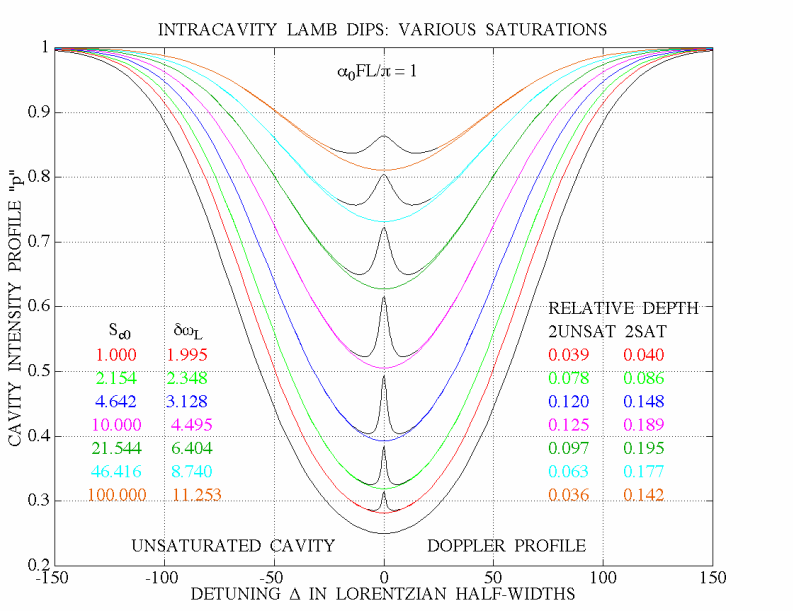

Figure 1.4. A Sequence of Intra-Cavity Lamb Dips Solved Using an Iterative Numerical Technique. The relative Lamb dip size reaches a maximum and then decreases. For this calculation, the absorption strength is roughly the same as the other cavity losses; expressed by the condition $\alpha_0 FL/\pi = 1$,, where α_0, F and L are unsaturated absorption coefficient, cavity finesse and length respectively.

small longitudinal velocities interact with both fields simultaneously. Being partially saturated by one field, the resulting absorption of the other is reduced, resulting in a dip with the shape of the homogeneously broadened line, far narrower than the Doppler line.

Figure 1.4 shows the effects on a spectral profile of saturation at various levels. For reference, an unsaturated profile is shown in black, being the deepest absorption feature. As the level of saturation S_{c0} increases, the Lamb dip depth increases to a maximum and then slowly decreases, both relative to the unsaturated and saturated Doppler profiles (labeled "RELATIVE DEPTH, 2UNSAT and 2SAT" in the annotation). The width of the Lamb dip also increases, shown here in relative line-width units, $\delta\omega_L$. However, the depth of the Doppler feature also decreases as saturation increases, resulting in less overall absorption.

As cavity finesse is increased in order to improve sensitivity, intra-cavity power easily becomes high enough to saturate typical LWIR small-molecule analytes. The resulting reduction in absorption clearly limits the effective sensitivity of the instrument. Our chosen method to alleviate this problem is to increase the sample detection pressure. Lamb dips appear at a particular set of conditions, and require low pressures such that collisional broadening is less that of the homogenous line-width. This unfortunately directly contributes to the saturation issue, as little will depopulate the relatively long-lived upper states. Increasing the pressure, depopulates these upper states alleviating saturation and deepening the Doppler absorption profiles, but washes out the Lamb dips.

The second limitation, which in fact compounds the first, is that we are heavily detector noise-limited, i.e., the dominant noise source is the detection process. This is especially true at high detection frequencies where the responsivity of the mercury-cadmium-telluride (MCT) detectors we use roll off to 35 dB less than the typical DC values. This drastically reduces the possible signal-to-noise ratios using the NICE-OHMS technique, and renders it approximately equivalent in sensitivity to our other best techniques. In addition, this also implies that we cannot reduce the impact of the saturation issue described above by reducing the power circulating in the cavity, as any gains in absorption sensitivity would be wiped out by decreasing signal-to-noise at the detector.

The third limitation involves the logistics and the modulation characteristics of the QCL. The NICE-OHMS technique requires the period of the RF modulation frequency to match the round-trip time of the optical cavity, which would require an optical cavity longer than 1.5 m to match a modulation frequency of less than 100 MHz. The requirement for logistically tolerable cavity lengths forces the use of modulation frequencies greater than 100 MHz. In the frequency range above 100 MHz, the QCL frequency modulation characteristics are poor and vary significantly from device to device. In this frequency range, adequate frequency modulation for NICE-OHMS is only possible at a peak in the FM characteristics. This peak is also narrow. Use of a cavity that was too long by 0.5 cm and the required modulation frequency change caused a difference in signal-to-noise ratio of 10 or more. It has also been demonstrated that the optimal modulation frequency is different from laser to laser. This clearly makes building a sensor based on this technique difficult. External modulation techniques have already been demonstrated impractical as the resulting devices finish by being larger and more power hungry than the others that we are already trying to miniaturize for the purposes of making fieldable equipment.

In light of these limitations our choice of architecture to proceed in the development of a fieldable sensor is either direct cavity transmission technique (the “Simple Cavity-Enhanced Sensor”), or the cavity-dither FM recovery technique, and target Doppler-limited spectroscopic features rather than sub-Doppler features. With the use of Doppler-limited features and operation with buffer gas pressures ~10 Torr, saturation should not be a problem, and cavity-enhanced sensors of high finesse should be able to operate successfully. High frequency modulation and response issues of both the QCLs and the MCT detectors are avoided, since the system will operate at tens of kilohertz rather than hundreds of megahertz. The detector elements can be larger, greatly alleviating the additional issues of alignment and optical fringing, discussed in the FY03 report.

1.3 Summary of Progress During FY04

The selection of a specific sensor architecture represents a new phase of experimental research and development. Until now, the focus of the experimental work was to demonstrate and explore the performance of the various architectures, and to identify and quantify the limitations of each technique. This was done without the need to select specific target chemicals, and consequently analytes were chosen more for convenience, ease of use and safety rather than for strategic importance. A major part of the work conducted in FY04 was to choose more strategic analytes, and molecular transitions. Implementing better gas handling systems and modifying laboratory systems to accommodate these analytes was also part of this work. In addition, a number of minor but time consuming technical issues

important for fieldable sensor design, but not critical for the first experimental phase, were delayed until this point. These included improving the alignment stability and mounting system of the QCL within the cryogenic dewar, and refining the drive electronics for the QCL. These are the issues we addressed during FY04, and will be discussed in detail in this report.

2.0 Selection of Test Molecules and Laser Wavelengths

The method for selecting suitable molecular species and transitions has been an iterative process involving our QCL supplier Maxion Technologies. Due to the large number of wavelength possibilities, in order expedite laser manufacture and delivery, it was necessary to streamline our QCL requirements by coordinating wavelength choices with other projects.

2.1 Selection of Test Molecules and Laser Wavelengths

In this section we discuss some of our choices for test molecules. Two database resources were used for this research, the first being Molspec, based on the Hitran database. The test conditions for spectra obtained from Molspec in this report were chosen to be 10 Torr analyte pressure corresponding to projected fieldable sensor operating pressure, a temperature of 296K, and over a path length of 16 cm as a desirable target cell length. Analyte concentration was chosen to be 1 part per million (ppm) as a standard test sample concentration. Standard impurities were chosen to include water at 1%, corresponding to a relative humidity of 35%, and carbon dioxide at 500 ppm. The second database used for this analysis is that being compiled by Steve Sharpe, the conditions for which are 1ppm-meter at 296K, taken at 1 atmosphere. All specified wavelengths are specified in vacuum.

2.1.1 Ammonia (NH_3)

Ammonia has been the chosen analyte of the short-wave infrared (SWIR) sensor being developed at PNNL by Richard Williams because it challenges gas-handling systems, and is representative of the physical and spectral characteristics of large categories of chemicals. Ammonia is a sticky molecule, and as such is typical of many analytes of interest, and demands that certain parts of the system be passivated with a glass layer in order to minimize absorption into the walls, and thus shorten both response and recovery times of the apparatus. We also chose ammonia in order to demonstrate the benefit of going to the LWIR due to the vastly increased absorption cross section at 9.5 micron as compared to 1.5 micron where the SWIR system operates. This is illustrated by the spectrum in Figure 2.1.

Warren Harper, who leads PNNL's FM Dial experiments, has extensively searched for an ammonia line clear of water interference, and has chosen 1046.39 cm^{-1} (9.557 μm). We will also use this line in order to utilize the same laser design implemented by Maxion, and facilitate rapid delivery. This chosen line is shown in Figure 2.2, ammonia lines being shown in magenta, and water lines in blue.

Note the considerable structure shown in the zoom of the ammonia line shown in Figure 2.2b. This structure makes the line easier to identify.

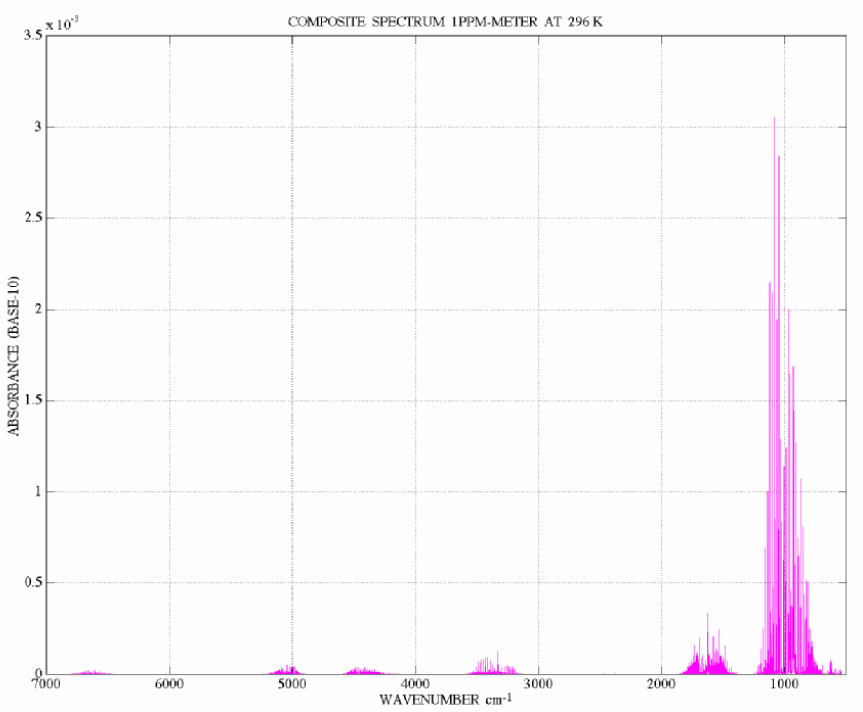

Figure 2.1. Spectrum of Ammonia Showing the Difference in Absorbance from the SWIR through to the LWIR

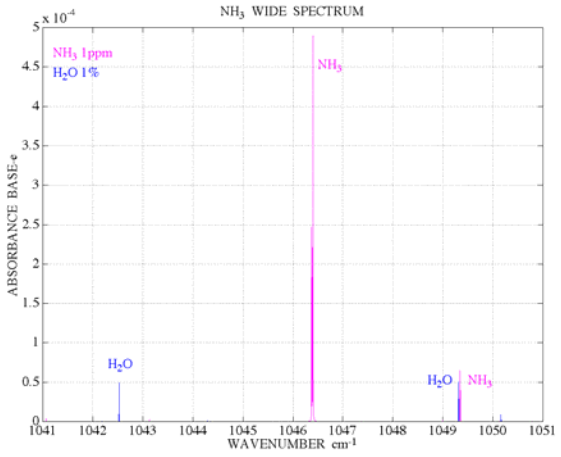

Figure 2.2a. FM Dial Choice of NH_3 Line at 1046.39 cm^{-1}. Water interference lines in blue – far from the line.

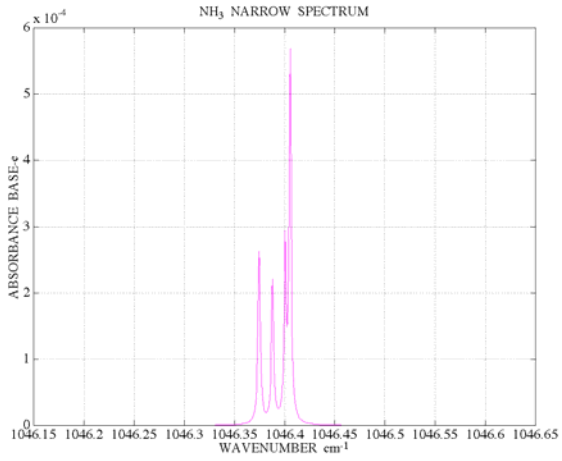

Figure 2.2b. A Zoom of this Line. Note the structure – useful as a signature.